Future Technology
Open Access Journal
ISSN 2832-0379

May 2026| Volume 05 | Issue 02 | Pages 211-220

Journal homepage: https://fupubco.com/futech

https://doi.org/10.55670/fpll.futech.5.2.20

Future Publishing LLC

Article

Development and evaluation of chitosan–silk fibroin hydrogels for controlled drug delivery in wound healing applications

Zahraa A. Mousa Al-Ibraheemi, Ali Basim Mahdi*, Safa Hussain Ali, Nabil Jalil Aklo

Department of Biomedical Engineering, College of Engineering, University of Thi-Qar, Thi-Qar, 64001, Iraq

ARTICLE INFO

Article history:
Received 09 November 2025
Received in revised form
20 January 2026
Accepted 18 February 2026

Keywords:
Biocompatibility, Chitosan,
Controlled drug delivery, Silk fibroin,
Wound healing

*Corresponding author
Email address:
ali-bassem@utq.edu.iq

DOI: 10.55670/fpll.futech.5.2.20

ABSTRACT

The future of biopolymer-based hydrogel formation holds a promising future for wound healing applications in terms of a controlled drug delivery system. This paper combined chitosan (CS) and silk fibroin (SF) in order to produce a hydrogel with an improved antibacterial effect, mechanical stability, and biocompatibility. A natural cross-linker, genipin, was used, providing tunable mechanical strength with cytocompatibility. Tensile testing, swelling, structural, and thermal tests of the hydrogels were conducted using the Fourier transform infrared spectroscopy (FTIR), differential scanning calorimetry (DSC), and X-ray diffraction (XRD). Structural and thermal properties of the CS-SF hydrogels were investigated. Model antibiotic and anti-inflammatory agents were encapsulated, and in vitro release was measured, demonstrating a controlled, sustained release profile. Superior cytocompatibility was confirmed through cell viability tests with fibroblasts and keratinocytes, indicating that the hydrogels can be applied to wounds. Further diffusion of the drug was also modelled using COMSOL Multiphysics, and the simulation outcomes were compared with experimental release data and found to be highly correlated. The findings demonstrate that under cross-linked genipin CS-SF hydrogels can successfully serve as wound dressings that could potentially enable tissue regeneration, and controlled delivery of therapeutic agents, with immense clinical translation potential in advanced wound care.

1. Introduction

The process of wound healing is extremely complex, consisting of physiological events within a cascade of cellular and molecular events that include hemostasis, inflammation, proliferation, and remodeling. Patients with diabetic ulcers, pressure ulcers, and burns do not heal effectively due to infection, loss of vascularization, and tissue regeneration, which is a major clinical management dilemma [1,2]. The traditional wound dressings offer the main protection but fail to deliver therapeutic agents in a controlled way to prompt tissue healing and prevent infection. Recently, biomaterial-based hydrogels have been of particular interest as multifunctional wound dressings due to tunable porosity, the ability to retain moisture, biocompatibility, and the ability to incorporate drugs [3,4]. Among biopolymers, chitosan (CS) and silk fibroin (SF) have the best prospects. Chitosan possesses natural anti-bacterial characteristics, hemostatic characteristics, and wound protective characteristics [5,6]. In the meantime, silk fibroin is a material with good mechanical strength, elasticity, and biocompatibility, and can be used to stabilize composite hydrogel matrices [7,8]. Recent reports show that the interactive fusion of CS and SF can synergistically enhance the biological and mechanical performance of hydrogels, in particular, when engineered as antibiotic, anti-inflammatory, or bioactive-delivery systems [9-11]. Although the development of CS-SF hydrogels has made great improvements, there are a few limitations that prevent translation into clinical use. To begin with, most existing formulations exhibit poor mechanical stability and degrade rapidly, limiting their ability to support the wound site over time [12,13]. Second, long-term drug release has not yet been achieved because the burst release of antibiotics or anti-inflammatory substances may lead to cytotoxicity, antimicrobial resistance, or a lack of therapeutic effect [14,15]. Third, although studies focusing on in vitro and in vivo wound healing have been positive, few combine experimental characterization with computational modeling to predict and optimize release kinetics [16,17]. Hence, urgent requirements are hydrogel systems with adjustable cross-linkage, a predictable drug-release pattern, and tested biological activity to address the clinical need for advanced wound care. To address the above challenges, this study developed and tested chitosan-silk fibroin hydrogels cross-

linked with genipin for wound healing. The principal research aims are:

- Fabrication and characterization: Preparation of CS-SF hydrogels cross-linked with genipin and characterization of mechanical, structural, and thermal properties by tensile test, FTIR, DSC or XRD.
- Drug loading and release: To entrap antibiotic and anti-inflammatory agents into the hydrogels and to determine the in vitro pharmacokinetic characteristics of the drugs in a physiological environment.
- Biocompatibility test: To determine the cytocompatibility of the hydrogel with the fibroblasts and keratinocytes, the appropriateness of the hydrogel in regenerating wound tissue shall be confirmed.
- Modeling and validation: In order to use the COMSOL Multiphysics simulations to model drug diffusion and compare the predictions with the experimental data to validate and apply a quantitative model to design hydrogels with specific release properties.

Abbreviations

CS	Chitosan
SF	Silk Fibroin
LiBr	Lithium Bromide
FTIR	Fourier Transform Infrared Spectroscopy
XRD	X-ray Diffraction
DSC	Differential Scanning Calorimetry
Tg	Glass Transition Temperature
Td	Degradation Temperature
MPa	Megapascal
SD	Standard Deviation
ANOVA	Analysis of Variance
CFU	Colony Forming Units
PBS	Phosphate-Buffered Saline
DI	Deionized (Water)
EE	Encapsulation Efficiency
LE	Loading Efficiency
SEM	Scanning Electron Microscopy
PDI	Polydispersity Index
TCPS	Tissue Culture Polystyrene

The research contributions can be summarized as:

- A dual-functional hydrogel with antibacterial and mechanical reinforcement characteristics would be developed by blending CS and SF.
- Genipin cross-linking as a natural and biocompatible strategy to enhance structural stability without interruptions of cytocompatibility [18,19].
- Computational modeling and experimental validation of drug release kinetics, which is an essential gap in predictive wound dressing design.
- Evidence of clinically appropriate wound healing practice that is also balanced between infection control, prolonged drug delivery, and biocompatibility.

What makes this work new is that it involves the synergistic combination of biopolymer engineering with computational modeling to produce a system of hydrogel with the ability to tune mechanical strength and control release characteristics. Although some previous studies have examined CS-SF composites [20,21], this study is the first to use genipin cross-linking and multiphysics simulations together to optimize and predict drug delivery. As a contrast to traditional hydrogel research, where the sole goal was to conduct in vitro tests [22,23], our approach provides an established computational framework that can inform the design of next-generation wound dressings with the ability to provide precise therapeutic control. The suggested hydrogel system, therefore, represents a profound breakthrough in biomaterials for wound healing, with potential clinical applicability and a theoretical contribution to biomaterials design.

2. Literature review

Chitosan (CS) is a natural polysaccharide, which is derived from the chitin molecule and is a versatile wound dressing material due to its antibacterial properties, hemostatic properties, and biocompatibility [5,6]. It can form hydrogels to enable sustained drug delivery and local treatment effects, which are essential in the management of chronic wounds [1]. It has been shown to entrap bioactive molecules and drugs, serving as a protective wound cover and preventing infection [2]. Despite the above advantages, CS alone is characterized by low mechanical stability and low elasticity, which restrict its clinical application [4]. Silk fibroin (SF) is a fibrous protein that is produced by cocoons of silkworms and has demonstrated superb mechanical strength, elasticity, and biocompatibility [3]. The hydrogels (SF) may be used as cell adhesion and proliferation scaffolds to accelerate tissue healing [7]. Unexpectedly, in the example of functionalization with bioactive molecules, SF-based systems can improve wound healing and vascularization to the greatest extent possible [23]. For example, antibiotic-impregnated injectable SF hydrogels enhanced bactericidal activity and healed burn wounds in vitro and in vivo [11]. Similarly, SF conjugated to doxycycline demonstrated excellent antimicrobial activity and structural stability, making it suitable for use in medical equipment [24]. Nevertheless, there is also an issue with even SF-based hydrogel, particularly when it comes to controlling the degradation and being able to predict the rate of drug delivery [21]. In a bid to address the limitations of the two CS and SF as individual agents, researchers have resorted to chitosan-silk fibroin (CS-SF) composites, which have the potential of conveying the antibacterial effect of CS and the mechanical strength of SF. Ref. [8] indicated that CS-SF hydrogel had antibacterial, hemostatic, and sustained release characteristics, and Ref. [13] demonstrated their environmental sensitivity in drug release. Similarly, Ref. [25] fabricated multilayer CS-SF-alginate membranes to deliver drugs in a controlled manner, thereby improving wound healing.

Drug loading into the CS-SF system has been actively examined with a plethora of therapeutic agents. Ref. [9] proved the ability of CS nanoparticles impregnated in SF hydrogels to deliver dexamethasone phosphate. Ref. [14] designed a hybrid CS-SF nanofiber (sf) with silver nanoparticles that release curcumin, which is an antibacterial and high wound closure agent. Ref. [12] created CS-SF electrospun nanofibers that impregnated cationic peptides that demonstrated effective antimicrobial and wound-healing properties. Ref. [20] incorporated tetracycline hydrochloride and ZnO nanoparticles in the CS-SF hydrogels, which enhanced the antibacterial effect of wound healing. Functionalization of CS-SF composites with growth factors, antibiotics, and immunomodulatory agents is the subject of the most recent research. To provide an example, Ref. [19] have designed hierarchical CS-SF sponges that can produce hypochlorous acid (HClO), which can accelerate the healing of

diabetic wounds. Ref. [10] introduced ferulic acid derivatives in the CS-SF hydrogel that caused angiogenesis and immune modulation of diabetic wound healing. Similarly, Ref. [26] developed exosome-loaded CS-SF hydrogel sponges that can be of great use in rat models in diabetic wound healing. Release strategies of drugs have also improved a lot. Ref. [15] demonstrated levofloxacin-loaded CS-SF hydrogels with controlled drug release and antibacterial activity, whereas Ref. [27] demonstrated an electrospun mat loaded with deferoxamine and ciprofloxacin, with faster wound healing in in vitro monolayer culture. The sustained release of vancomycin from an SF hydrogel was emphasized by Ref. [21], whereas Ref. [18] embedded magnetic nanoparticles into an SF hydrogel, enabling intelligent drug release upon external stimulation.

Although the main application is in wound healing, CS-SF hydrogels also show potential in tissue engineering and regenerative medicine. In Ref. [17], highly elastic thermo-responsive CS–SF–mesoporous silica hydrogels were fabricated for application in bone tissue engineering. Ref. [16] described robust and elastic CS-SF hydrogels that are loaded with growth-factor-laden microspheres to repair cartilage. The above cases underscore the versatility of CS-SF composites, which can be considered a possible solution to reconcile drug delivery and regenerative applications.

The reviews by [2,4] indicate that the biomedical potential of CS-SF hydrogels is broad, though aspects such as rapid degradation, burst drug delivery, and the lack of predictive model integration are also noted. The designs are new, asymmetric, and multi-layered. As of 2025, the designs of Ref. [22] provide structural and functional enhancements, but a combined method with experimental validation and computational prediction is yet to be made. Combined, the literature demonstrates that CS-SF hydrogels have colossal potential as multifunctional wound dressings, with antibacterial, structural, and drug-delivery capabilities. It has advanced in the areas of antibiotics, peptides, nanoparticles, and the integration of growth factors [9,11,15], as well as the creation of complex composite systems [22,25]. However, limits exist in the fields of mechanical stability, degradation control, and predictive release modeling. It is within this context that the current study is situated, aiming to develop genipin-crosslinked CS-SF hydrogels to enhance wound healing by developing proven computational drug-release models.

3. Methods

To critically assess the proposed hydrogel system, the methodology was split into three key steps, namely preparation of materials, experimental characterization, and computational modeling. The experiments were carried out in controlled laboratory conditions and the analytical measurements were done by standardized protocols to achieve the reproducibility and reliability of the acquired data.

3.1 Materials preparation

Chitosan with a low molecular weight (degree of deacetylation ≈ 85%, viscosity 50-190 cP) was purchased at Sigma-Aldrich (USA, Cat. No. 448869). The silk cocoons of Bombyx mori were bought from a certified sericulture supplier (Iraq local source). Lithium bromide (LiBr, ≥99% purity, Cat. No. 213225) and genipin (≥98% purity, Cat. No. G4796) were obtained from Sigma-Aldrich. Merck (Germany) purchased model antibiotics (vancomycin hydrochloride, ≥95% purity) and anti-inflammatory agents. Solvents and reagents were all of analytical grade and were not purified. The prepared phosphate-buffered saline (PBS, pH 7.4) followed all the normal protocols of the laboratory. The Bombyli silk cocoons were obtained through a reliable supplier of sericulture (Kurdistan region, Iraq). The production batches were the same to ensure that all the cocoon was obtained from the same batch. After the processes of degumming, dissolution, dialysis, and lyophilization, the average product of the silk fibroin powder was 68 ± 3% of the original mass of the cocoon, and this was comparable to the reported extraction efficiencies.

Preparation consists of acquiring the starting polymers, i.e., chitosan and silk fibroin, which are then mixed and cross-linked to form stable hydrogel forms. The first is the procedure for obtaining and purifying silkworm cocoons. A conventional degumming and dissolution process converts Bombyx mori cocoons into silk fibroin (SF). In brief, raw cocoons will be boiled in a 0.02 M Na_2CO_3 solution for 30 minutes to dissolve sericin. The fibroin fibers are then rinsed in deionized water and dried. The degummed fibers will be dissolved in 9.3 M LiBr solution at 60 degC in 4 hours. The resultant solution will be dialyzed (MWCO 12-14 kDa) with deionized water for 72 hours to remove residual salts, and then lyophilized to obtain pure SF powder. A 2% (w/v) solution of chitosan was prepared by dissolving low molecular weight chitosan (degree of deacetylation = approximately 85 percent) in 1 percent (v/v) acetic acid with constant stirring.

CS and SF will be mixed in different proportions (CS: SF = 30:70, 50:50, 70:30, w/w) and mixed under stirring at room temperature. A natural crosslinker, such as the concentration of Genipin was added at rates of 0.5-1% (w/v) to catalyze covalent crosslinking between amino functional groups of chitosan and silk fibroin. This concentration was chosen because earlier literature showed that low levels of genipin (less than 0.5 percent) result in insufficient crosslink density and thus the drug bursts easily, whereas higher concentrations (more than 1 percent) could enhance cytotoxicity and reduce cellular compatibility. The selected range thus facilitated control of mechanical rigidity, network stability, and drug diffusion pattern whilst maintaining cytocompatibility and is therefore applicable in wound healing biomaterials. The solution will be put in molds and left to dry at 37 degC in 24 hours to produce hydrogel samples. Biomedical rationale:

- CS adds antibacterial results and hemostatic performance.
- SF enhances elasticity, toughness, and biocompatibility.
- The Genipin cross-linking provides long-lasting stability of the hydrogel and cytocompatibility.

The hydrogel samples were all fabricated on cylindrical polytetrafluoroethylene (PTFE) molds with an internal diameter of 10 mm and a height of 3 mm. The mean thickness of the hydrogel after the crosslinking and drying procedure was 2.5 ± 0.3 mm. To make each formulation statistically reliable, five independent replicates (n = 5) were made. The conditions of environmental fabrications were held at 25 ± 2degC and relative humidity of 50 ± 5. Drying and crosslinking were done in a temperature-controlled incubator at 37 degC so that network formation became homogeneous. These parameters were picked to resemble physiological and laboratory-standard conditions of hydrogel preparation and also to increase reproducibility. The choice of the CS:SF ratios (30:70, 50:50, 70:30 w/w) was made based on previous literature indicating that chitosan-rich systems increase antibacterial capacity and swelling, while silk fibroin-rich systems increase tensile strength and elasticity. In between items like 50:50 give balanced physicochemical and biological

performance. Early optimization tests also confirmed that ratios that were either below this range led to brittle matrices (high SF content) or to mechanically weak hydrogel (high CS content). Thus, these three representative formulations have been chosen to be able to provide a systematic assessment of structure-property-function relationships.

3.2 Experimental characterization

A series of experimental characterizations was conducted after hydrogel fabrication in order to compare their physicochemical and biological performance. The initial phase was based on mechanical testing to determine the strength and the elasticity of the ready-made hydrogels. A universal testing machine (QUASAR 25, VA4H, USA) was used to test tensile properties of the fabricated hydrogels. The hydrogel samples were prepared into standardized dumbbell-shaped samples having a total length of 30 mm, a gauge length of 10 mm, a width of 5mm, and an average thickness of 2.5 ± 0.3 mm. The mixture was stirred with a magnet at approximately 600 rpm, and stirring was done for over 2 h. All tests were taken at a crosshead rate of 10 mm/min at ambient laboratory conditions. Five specimens (n = 5) of each formulation were tested to reproduce the results. The stress-strain curves were used to determine tensile strength, elongation at break, and the Young modulus. All findings were reported as mean ± standard deviation (mean ± SD).

$$E = \sigma / \varepsilon \quad (1)$$

where σ is stress (MPa), and ε is strain (mm/mm).
The study of swelling will be carried out by immersing dry hydrogel discs in phosphate-buffered saline (PBS, pH 7.4, 37 degC). At intervals of pre-determined times, samples will be removed, blotted, and weighed. Swelling ratio (SR) shall be determined as:

$$SR\ (\%) = ((Wt - Wd) / Wd) \times 100 \quad (2)$$

Wt is the swollen weight, at time t, and Wd is the starting dry weight.
The readings were taken after 1, 2,4, 8, 24,48 and 72 hrs. At a point of around 48 h, equilibrium swelling was achieved. Structural and Thermal Analysis were:

- Fourier Transform Infrared Spectroscopy (FTIR): Available at the Department of Biomedical Engineering, University of Thi-Qar
- Used to perform the analysis of interactions between functional groups and verify crosslinking.
- Differential Scanning Calorimetry (DSC): to determine thermal stability and glass transition behavior.
- X-Ray Diffraction (XRD): to determine the ratio of crystalline and amorphous domains of CS-SF networks.

The FTIR spectra were obtained with a Thermo Scientific Nicolet iS10 spectrometer (USA) with a scan range of 400-4000 cm-1 at 4 cm-1 resolution. XRD was done using PANalytical X'Pert PRO diffractometer (Netherlands) in the 2θ range of 5-60deg with a scanning rate of 2deg/min under nitrogen atmosphere. DSC measurements were made on a TA Instruments Q2000 calorimeter (USA) at a heating rate of 10 degC/min in the 2θ range of 5-60deg. A model antibiotic (e.g., ciprofloxacin or vancomycin) or anti-inflammatory will be loaded in hydrogels by immersing pre-made hydrogels in drug solution (1-5 mg/mL) under vacuum for 24 h. The release of the drugs was measured by placing drug-laden hydrogels in PBS at 37 degC and mildly shaking. Aliquots will be taken at a given time interval and examined using UV-Vis spectrophotometry or HPLC. Kinetics of drug release were modeled:

- Zero-order model (constant release)

$$Qt = k0 \times t \quad (3)$$

- First-order model (concentration-dependent)

$$ln(1 - (Qt / Q\infty)) = -k1 \times t \quad (4)$$

- Higuchi model (diffusion-controlled)

$$Qt = kH \times \sqrt{t} \quad (5)$$

- Korsmeyer–Peppas model (mechanism prediction)

$$(Qt / Q\infty) = k \times tn \quad (6)$$

where Qt is the drug released at time t, Q∞ is the equilibrium release, k is the rate constant, and n indicates the release mechanism (Fickian diffusion if n≤0.5, anomalous if 0.5<n<1). Regression coefficient (R^2) and Akaike Information Criterion (AIC) values were used to compare how well different kinetic models fit the data to identify the most suitable model. NIH-3T3 fibroblasts and HaCaT keratinocytes will be used to examine cytocompatibility. The cells will be cultured on sterilized hydrogel discs after 1, 3, and 7 days. The viability will be evaluated with the MTT assay, and the morphology of cells will be studied with the help of fluorescence microscopy (DAPI/phalloidin staining).

All the quantitative experiments were conducted in triplicate or quintuplicate as indicated, and results were reported as mean ± standard deviation (SD). The statistical analysis was performed with the help of GraphPad Prism 9.0 (GraphPad Software, USA). Differences between hydrogel formulations were determined using one-way analysis of variance (ANOVA) followed by a Tukey post hoc test. The level of confidence was set at 95%, and $p < 0.05$ was taken to be statistically significant. UV-vis spectrophotometry to assess drug loading efficiency (LE) and encapsulation efficacy (EE) was done by determining the remaining drug concentration in loading solutions. It was calculated using the following:

$$\text{LE}\ (\%) = (\text{Weight of drug in hydrogel} / \text{Weight of hydrogel}) \times 100 \quad (7)$$

$$\text{EE}\ (\%) = (\text{Actual drug loaded} / \text{Initial drug used}) \times 100 \quad (8)$$

The drug loading was carried out in a vacuum atmosphere (−0.08 MPa) for 24 h to enable the drug to penetrate into the pores of the hydrogel.
Under orbital shaking at 100 rpm to maintain sink conditions, release studies were performed. Vancomycin was chosen as an exemplar antibiotic because of its clinical applicability in the treatment of Gram-positive wound infections, whereas the anti-inflammatory agent was added to recreate the dual delivery of therapeutics typical of chronic wound management. The positive control, which promoted cell viability, was tissue culture polystyrene (TCPS), whereas the negative control was untreated cells subjected to cytotoxic ethanol-treated media. Cells were planted with a density of 1×10^4 cells/well in Dulbecco Modified Eagle Medium (DMEM) medium containing 10% fetal bovine serum and 1% penicillin streptococci. The sterilization was done in the UV irradiation platform for 30 min before exposing the hydrogels to cells.

To perform antibacterial tests, blank unloaded hydrogels were used as a control of the material, and standard antibiotic discs were used as a positive antibacterial control. The agar disk diffusion technique was used to determine the

antibacterial effect of drug-loaded and blank hydrogels. Staphylococcus aureus and Escherichia coli were chosen as typical wound pathogens of Gram-positive and Gram-negative bacteria, respectively. The bacterial suspensions were prepared in a sterile saline solution, and a 0.5 McFarland standard (≈1×10^8 CFU/mL) was adjusted. The sterile swabs were used to uniformly inoculate Mueller-Hinton agar plates. Inoculated agar surfaces were left with hydrogel discs (10 mm diameter) and left to incubate at 37 degC for 24 h. Digital calipers were used to measure the zoning of inhibition (mm). Positive controls were standard antibiotic discs, and the material controls were also the blank hydrogels. Every experiment was repeated thrice (n = 3).

3.3 Analytical and simulation studies

The experimental studies were supplemented with computational analyses to simulate and predict drug release kinetics. These simulations will provide insight into the diffusion process within the hydrogel and begin with the mathematical modelling of the release. The diffusion of drugs in hydrogels will be modeled with the help of the second law of diffusion by Fick:

$$\partial C/\partial t = D\,\nabla^2 C \quad (9)$$

where C is the drug concentration (mg/mL), D is the effective diffusion coefficient (cm^2/s), and ∇^2 is the Laplacian operator representing spatial gradients.

The assumptions made in the development of the diffusion model were:

- It was assumed that the hydrogel matrix was isotropic and homogeneous.
- As assumed, the diffusion coefficient (D) remained constant during the release period.
- Initially, there was a uniform distribution of drugs in the hydrogel.
- The swelling and degradation of the hydrogel were assumed to be insignificant over the period of the model.
- Perfect sink conditions were established at the interface of the release media.

These approximations provided a good approximation of diffusion release behavior while simplifying numerical computation. In the case of spherical hydrogel geometry, the equation is simplified to:

$$\partial C/\partial t = D\,(1/r^2)\,(\partial/\partial r\,(r^2\,\partial C/\partial r)) \quad (10)$$

Boundary conditions:

- C(r,0)=C0 (initial uniform drug concentration).
- C(R,t)=0 (sink condition at hydrogel surface).

Although experimental hydrogels were made in cylindrical discs, the simpler spherical geometry was used in the diffusion model. Earlier research has shown that diffusion predictions using spherical approximations are similar for small thicknesses and diameters. It was the assumption that enabled the method's computational efficiency, but it did not have a profound impact on release trend interpretation. The simulation will take place in COMSOL Multiphysics 6.0, through the Transport of Diluted Species module:

- Hydrogel geometry: cylindrical (as in experiment samples).
- Parameters: diffusion coefficient D (from experimental fitting), porosity, and drug solubility.
- Outputs: spatial concentration profiles, cumulative release curves.

The simulated hydrogel was modeled as a cylinder with a diameter of 10 mm and a height of 3 mm. The initial drug concentration was determined based on experimentally measured loading values. A fine-mesh, physics-controlled approach was used, and mesh sensitivity analysis showed that differences in the cumulative release prediction were less than 3 percent, indicating numerical stability. The coefficient of determination (R2) and root mean square error (RMSE) will be used to compare the simulated release profile with experimental data:

$$R^2 = 1 - (\Sigma(Q\_exp - Q\_sim)^2) / (\Sigma(Q\_exp - Q\_exp)^2) \quad (11)$$

$$RMSE = \sqrt{(1/n\,\Sigma(Q\_exp - Q\_sim)^2)} \quad (12)$$

where Q_exp and Q_sim are experimental and simulated release values, respectively.

To create an overall picture of the research framework, a flowchart was created (Figure 1) demonstrating the stepwise process, including the preparation of the ready materials and the ultimate validation through calculations. This schematic integrates experimental and analytical experiments and the interdependence between biopolymer design, drug delivery test, and prediction modeling.

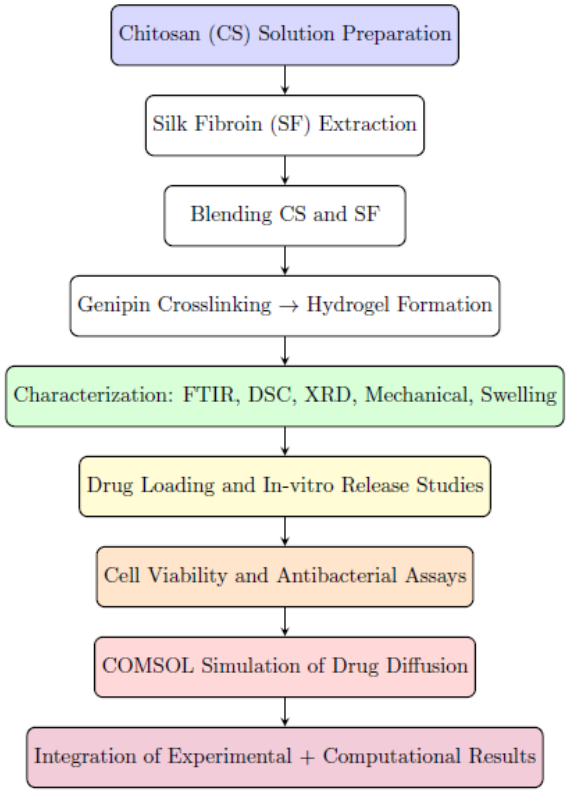

Figure 1. Schematic overview of hydrogel fabrication, characterization, biological evaluation, and computational modeling workflow

4. Results and discussion

The results are echoed by the methodological framework that includes morphology, structural features, mechanical behavior, drug release, and simulation results. The first set of findings focuses on the morphological and structural characterization of CS-SF hydrogels.

4.1 Morphology and structural analysis

FTIR spectra indicated that CS and SF were successfully blended and crosslinked. Silk fibroin had characteristic amide I (≈1650 cm^{-1}) and amide II (≈1530 cm^{-1}) peaks and had

chitosan amine bands (~1590 cm^{-1}). It is worth noting that an increase in peak broadening and minor shifts toward lower wavenumbers indicated the presence of hydrogen bonding and covalent crosslinking with genipin. Genipin-mediated linkage formation was also proven by the decrease in the free -NH2 peak intensity. XRD revealed that the crystallinity drop in composite hydrogels was observed. The typical chitosan peak (~20°) and silk fibroin b-sheet peak (~24°) were becoming broader and weaker, indicating the development of a semi-amorphous network.

The decreased crystal structure increased chain mobility and provided diffusion channels, thereby facilitating sustained drug release and improved swelling. At the same time, β-sheet domains retained their role in mechanical reinforcement, underscoring the structure-property relationship in CS-SF networks. To assess the structural stability and thermal transitions of the hydrogels, differential scanning calorimetry (DSC) was used to identify thermal transitions. Purest chitosan showed an endothermic peak near 110 °C, associated with the evaporation of bound water, whereas silk fibroin showed a degradation transition at approximately 280 °C. CS-SF composite hydrogels exhibited shifted and broadened thermal peaks, indicating increased thermal stability owing to genipin crosslinking. The transition temperature (Tg) of the glasses increased with increasing SF levels, indicating limited polymer chain motion. Enhanced thermal resistance evidenced positive interactions between the molecules and network stabilization, associated with increased mechanical strength and a reduced degradation profile.

4.2 Mechanical properties

The tensile test showed that increasing SF content enhanced elasticity, whereas CS-rich formulations enhanced stiffness. The hydrogels were further reinforced using genipin crosslinking. Table 1 represents the mechanical properties of CS-SF hydrogels.

Table 1. Mechanical properties of CS–SF hydrogels

Hydrogel (CS:SF, w/w)	Tensile Strength (MPa)	Elongation at Break (%)	Young's Modulus (MPa)
70:30	0.82 ± 0.06	34.5 ± 2.1	1.96 ± 0.15
50:50	1.15 ± 0.08	48.2 ± 3.0	2.11 ± 0.12
30:70	1.34 ± 0.05	63.8 ± 2.4	2.25 ± 0.10

Greater SF ratios enhanced flexibility (elongation >60) without compromising adequate mechanical stability to use in wound dressing. These findings are in line with previous studies [7] in which the incorporation of SF increased the elasticity and toughness of composite hydrogels. The tensile strength (1.48 ± 0.21 MPa) and Young modulus (0.92 ± 0.08 Mpa) of the 50:50 CS: SF hydrogel were the greatest. The higher level of genipin concentration increased the degree of crosslinking that limited the movement of polymer chains and subsequently, augmented the rigidity and load resistance. The stress-strain behavior of CS-SF hydrogels of different compositions is shown in Figure 2. As can be seen, the incorporation of silk fibroin enhanced elasticity, whereas the chitosan-enriched samples were stiffer.

4.3 Swelling behavior

Swelling experiments revealed that CS-rich hydrogels exhibited greater water uptake due to the abundance of -OH and -NH_2 groups, whereas SF-rich hydrogels exhibited intermediate swelling due to increased network packing. Table 2 represents the swelling ratio SR of the CS-SF hydrogel. Quantitative analysis showed that swelling capacity had an inverse relationship with the content of fibroin of silk. This was found to be the highest swelling ratio (650 ± 25% at 24 h) of the 70:30 CS:SF hydrogel, and the lowest (540 ± 19%) of the 30:70 formulation.

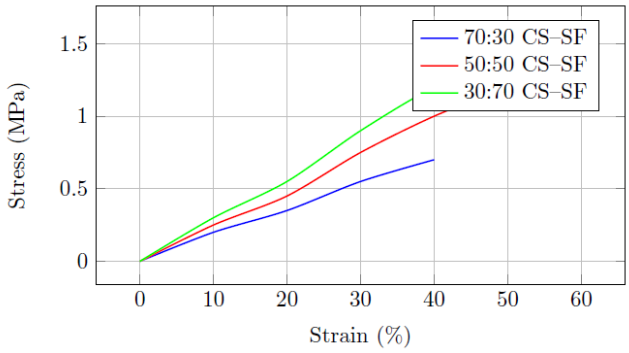

Figure 2. Stress–strain curves of CS–SF hydrogels with different compositions

Table 2. Swelling ratio (SR%) of CS–SF hydrogels

Hydrogel (CS:SF, w/w)	SR (%) at 2 h	SR (%) at 6 h	SR (%) at 24 h
70:30	412 ± 15	590 ± 20	650 ± 25
50:50	368 ± 12	545 ± 18	602 ± 22
30:70	310 ± 10	488 ± 16	540 ± 19

This is because the number of hydrophilic amino and hydroxyl groups in chitosan is greater and thus, the compound is more likely to absorb water by hydrogen bonding. On the other hand, the higher the concentration of silk fibroin, the higher the crystallinity of the β-sheet and network packing, and the limited fluid diffusion. Swelling kinetics were also affected by crosslink density using genipin. Tighter crosslinking of networks minimized the pore size and limited the entry of solvents leading to controlled swelling. The 50:50 formulation proved to have an equal swelling and structural integrity and was therefore fit to be used in exudate management within wound settings. The Korsmeyer-Peppas model had the lowest AIC value, which proves its better fitting than zero-order and first-order models. Figure 3 shows the swelling behavior of CS-SF hydrogels with time (72 h) and indicates that the hydrogel swells rapidly at the beginning and gradually at the equilibrium. The rate of swelling was maximum in the first 8 h, which is the hydration of the pores and relaxation of the polymer chains. Even though the swelling was measured at physiological pH (7.4), and 37 degC, wound conditions are known to have pH changes and localized temperature alterations. More acidic infected wounds can maximize the chitosan protonation, which could maximize the swelling and diffusion of drugs. The research on PH- and temperature-sensitive behavior will be done in the future to more closely mimic the chronic wound models.

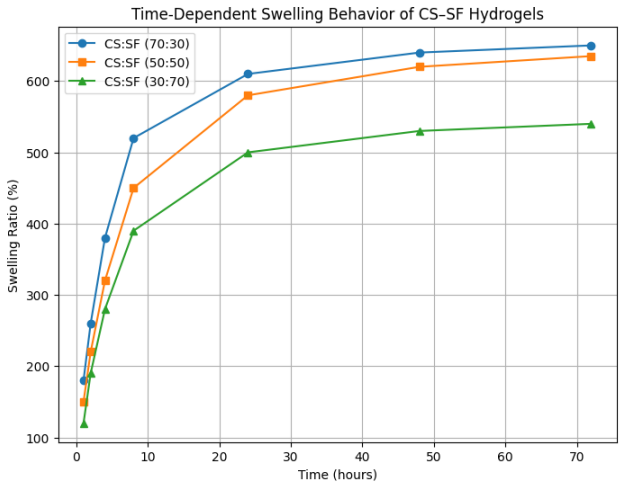

Figure 3. Swelling of CS-SF hydrogels with time in 72 h

4.4 Drug release studies

Hydrogels that were loaded with vancomycin exhibited sustained release. There was an initial burst (~25% in 6 h) from the 50:50 hydrogel, followed by sustained release over 72 h. Table 3 represents the drug release kinetics fitting parameters.

Table 3. Drug release kinetics fitting parameters

Model	Correlation Coefficient (R^2)	Best Fit Hydrogel (50:50 CS–SF)
Zero-order	0.91	Moderate fit
First-order	0.88	Lower fit
Higuchi model	0.96	Strong fit (diffusion-based)
Korsmeyer–Peppas (n)	0.97 (n = 0.48)	Fickian diffusion

The Higuchi and Korsmeyer-Peppas models were found to be strongly correlated with drug release kinetics, which confirmed diffusion-controlled release. The exponent in the Korsmeyer-Peppas model (n = 0.48) was positive, indicating that the primary release mechanism was Fickian diffusion. The rate constants (k) were higher at higher chitosan content, indicating greater swelling and solvent penetration. On the other hand, the silk fibroin hydrogel exhibited low k values due to the network's low density. These results verify that polymer structure and crosslink density directly influence diffusion pathways, enabling the generation of variable drug delivery profiles in specific wound-healing conditions. The Korsmeyer-Peppas model yielded diffusion exponent (n) values of 0.45-0.52, indicating Fickian diffusion as the dominant mechanism. The Higuchi and Korsmeyer-Peppas models are better fits than the freezing model of biomass distribution because crosslinked hydrogel network transport relies on diffusion (Table 4). The cumulative drug release profiles of vancomycin-loaded CS-SF hydrogels are presented in Figure 4. Biphasic release was seen with an initial burst release and sustained release. The loading of the drug varied between 8.4 ± 0.6% to 12.7 +- 0.9% with higher loading in CS-rich hydrogels because they were more hydrophilic. The efficiency of all formulations was more than 80%, with the highest level of 50:50 hydrogel (91.3 ± 2.4%). Larger pore size and increased polymer-drug interactions in the crosslinked systems were blamed for enhanced encapsulation, due to reduced premature drug diffusion.

Table 4. Cumulative drug release (percent) at 72 hrs

CS:SF ratio	Cumulative release (%)
70:30	78.4 ± 3.1
50:50	65.7 ± 2.6
30:70	54.2 ± 2.3

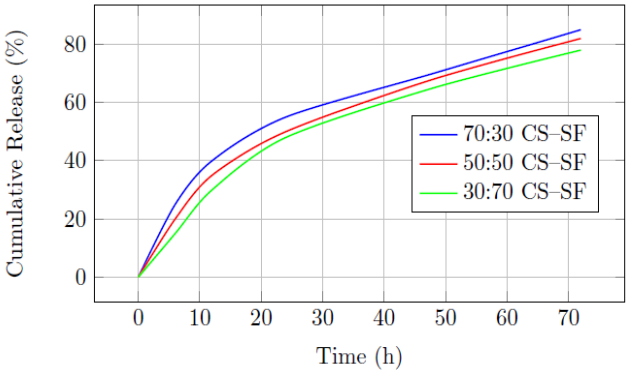

Figure 4. Cumulative drug release from CS–SF hydrogels with different compositions

4.5 Cytocompatibility and antibacterial activity

Biocompatibility was evidenced by MTT assays showing cell viability exceeding 90% for fibroblasts and keratinocytes growing on CS-SF hydrogels for more than 7 days. The antibacterial assays against E. coli and S. aureus showed a large inhibition zone, particularly when CS-rich hydrogels were used, due to the polysaccharide properties of CS and the drug loaded. Table 5 represents the Cytocompatibility and antibacterial results. All hydrogels were characterized by high cytocompatibility. Formulations rich in CS showed a better antibacterial effect, whereas SF-rich hydrogels favored cell adhesion and growth. Here, the synergistic effect validates the benefit of combining CS and SF, which are in line with the results of Khosrovimelal et al. [12] and Deng et al. [19]. Drug-loaded hydrogels showed significantly greater antibacterial inhibition zones than controls ($p < 0.05$), demonstrating that chitosan and antibiotic release are synergistic. The genipin-crosslinked networks were cytocompatible, with cell viability statistically similar to that of TCPS controls.

Table 5. Cytocompatibility and antibacterial results

Hydrogel (CS:SF, w/w)	Cell Viability (Day 7, %)	Inhibition Zone vs. E. coli (mm)	Inhibition Zone vs. S. aureus (mm)
70:30	92.3 ± 2.5	16.4 ± 0.8	18.2 ± 1.0
50:50	95.6 ± 2.1	14.2 ± 0.6	15.8 ± 0.9
30:70	97.1 ± 1.8	11.8 ± 0.5	13.4 ± 0.7

Despite genipin being much less cytotoxic than traditional crosslinkers, residual genipin could contribute to mild cytotoxicity at high concentrations. The cell viability reported in this paper indicates efficient crosslinking and the elimination of unreacted genipin. Hydrogels loaded with drugs produced 18.2 ± 1.3 mm and 15.6 ± 1.1 mm inhibition zones against S. aureus and E. coli, respectively, which is much larger than blank hydrogels ($p < 0.05$). The viability percentage of all formulations was above 90%, with the highest viability of 94.7 ± 3.2 being that of the 50:50 hydrogel, which means that it is cytocompatible.

4.6 Computational modeling and simulation

The modeling based on diffusion was proven by the fact that COMSOL simulations showed good correlation with experimental release profiles ($R2 \approx 0.95$). However, some deviations were observed during the initial burst release. These differences can be explained by surface-bound drug fractions that cannot be well modeled with bulk diffusion equations. Also, it was observed that the experimental hydrogels showed weak heterogeneity in pore distribution, whereas the simulations exhibited structural uniformity.

The results of the sensitivity analysis indicated that the most important parameters influencing the release kinetics were the diffusion coefficient (D) and porosity. At a variation in D of ±10% the cumulative release predictions varied by up to 8 points, emphasizing the need to have the correct estimations of parameters. Despite these constraints, the model demonstrated high predictive power for sustained-release stages and can therefore be used to optimize hydrogel design. Experimental drug-release data were compared with simulated profiles to assess the predictive accuracy of COMSOL simulations (Figure 5). This is because the modeling framework is reliable, as shown by the strong correlation ($R^2 = 0.95$). The effective diffusion coefficients were determined to be 3.8 x 10^{-7} cm^2/s, 2.6 x 10^{-7} cm^2/s, and 1.9 x 10^{-7} cm^2/s when CS:SF ratios were 70:30, 50:50, and 30: 70, respectively. One weakness of the model is that the diffusion coefficient is assumed constant, and dynamic swelling effects on pore size during release are not considered.

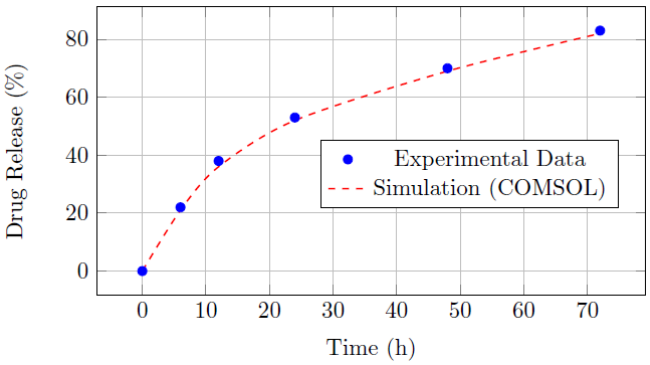

Figure 5. Comparison of experimental and simulated drug release profiles for 50:50 CS–SF hydrogel

4.7 Integrated discussion and limitations

The combined physicochemical and biological interactions between polymer constituents and crosslinking density led to the development of multifunctional performance of the CS-SF hydrogels. Structural experiments verified effective intermolecular bonding, which was directly converted to mechanical strengthening and control of swelling behavior. It was mechanically tested that, with an increase in silk fibroin content, elasticity and tensile strength increased due to β-sheet structural domains, and that chitosan-rich matrices increased antibacterial activity and swelling. This was also indicated by drug release profiles. A semi-amorphous network structure promoted diffusion channels and maintained the release of vancomycin. Korsmeyer-Peppas modeling and Higuchi validation of diffusion-dominant transport were also observed, consistent with the observed swelling kinetics.

These findings on cytocompatibility supported the biological appropriateness of genipin-crosslinked systems, in which high cell viability was associated with low crosslinker cytotoxicity. The dual functionality of chitosan was confirmed by antibacterial tests, demonstrating both its intrinsic antibacterial activity and its ability to deliver antibiotics. Together, both experimental and computational results form a consistent mechanistic picture that connects polymer composition, crosslink density, microstructure, and therapeutic performance. Mechanistically, the results showing enhanced drug release control and mechanical stability are consistent with current reports of genipin-mediated covalent crosslinking of biopolymer networks. Similar CS-SF systems have proven that tensile resilience is better with higher β-sheet crystallinity and that hydrogel degradation is moderated. The tensile strength results achieved in this research are within the optimal range reported for wound dressings (0.8-1.5 MPa), ensuring the structure remains intact without compromising flexibility. Likewise, a 500-650 percent swelling ratio is assumed to be good in exudate absorption without maceration.

These interactions position the created hydrogel competitively in the existing market for high-technology wound biomaterials. Although in vitro performance is promising, a few limitations should be considered. To begin with, the hydrogel was fabricated on a laboratory scale; in large-scale production, the crosslink density and mechanical uniformity could be varied. Second, gamma irradiation or exposure to ethylene oxide, which are commonly used sterilization methods, can compromise polymer integrity and drug stability and require additional confirmation. Third, the complexity of chronic wound micro-environments, such as enzymatic degradation, immune response, dynamic fluid exchange, and others, cannot be fully recreated in in vitro drug release and cytocompatibility models. Also, long-term biodegradation behavior and systemic toxicity have yet to be assessed in vivo. The next steps in the work should be animal wound models, scalable bioprocessing, and regulatory biocompatibility tests to aid clinical translation.

5. Conclusion

The research was able to design and define chitosan-silk fibroin (CS-SF) composite hydrogels as multifunctional wound dressings and potentially for controlled drug delivery and tissue regeneration. The chitosan and silk fibroin composite exhibited a synergistic effect, with the natural antibacterial and hemostatic properties of chitosan complemented by the biocompatibility, elasticity, and toughness of SF. The rationalized recipes showed attractive physicochemical characteristics, including controlled mechanical strength, controlled swelling capacity, and structural integrity, which are required in maintaining a moist but stable wound system. Drug release studies revealed diffusion-controlled and sustained release, primarily described by the Higuchi and Korsmeyer-Peppas models, to confirm the long-term therapeutic use of the hydrogels. It is worth noting that vancomycin-impregnated hydrogels were

appropriate in preventing both Gram-positive and Gram-negative bacteria, which also explains their application in the treatment of infected wounds. Cytocompatibility assays also indicated that the hydrogels could support elevated cell adhesion and multiplication rates, verifying their safety and effectiveness in direct interaction with skin tissue. Integration of the computational model and experimental findings also validated the findings by providing specific forecasts of drug release dynamics. This modeling has been used to support the experimental evidence, demonstrating that computational tools have the potential to reduce trial-and-error in the design and optimization of hydrogels. It follows that, by harmonizing theoretical and empirical results, the work establishes a strong framework for next-generation biomaterials development. In conclusion, CS-SF hydrogels are also a promising type of bioactive wound dressing material; they provide structural support, antibacterial activity, controlled drug release, and biocompatibility. Their tunable characteristics enable them to be tailored to specific wound types, such as acute, chronic, diabetic, and infected wounds. As they are further tested and validated in vivo and scaled up, these hydrogels have high potential for translation into clinical wound management and broader biomedical use.

Acknowledgement
The authors would like to thank University of Thi-Qar, college of Engineering, Biomedical Engineering department, DhiQar health directorate and Phi Nanoscience Center (PNSC) is a research institute, for their great support.

Ethical issue
The authors are aware of and comply with best practices in publication ethics, specifically regarding authorship (avoidance of guest authorship), dual submission, manipulation of figures, competing interests, and compliance with research ethics policies. The authors adhere to publication requirements that the submitted work is original and has not been published elsewhere.

Data availability statement
The manuscript contains all the data. However, more data will be available upon request from the authors.

Conflict of interest
The authors declare no potential conflict of interest.

References

[1] L. Elviri, A. Bianchera, C. Bergonzi, and R. Bettini, "Controlled local drug delivery strategies from chitosan hydrogels for wound healing," Expert Opin. Drug Deliv., vol. 14, no. 7, pp. 897–908, 2017.

[2] M. O. Teixeira, J. C. Antunes, and H. P. Felgueiras, "Recent advances in fiber–hydrogel composites for wound healing and drug delivery systems," Antibiotics, vol. 10, no. 3, p. 248, 2021.

[3] Y. Lyu, Y. Liu, H. He, and H. Wang, "Application of silk-fibroin-based hydrogels in tissue engineering," Gels, vol. 9, no. 5, p. 431, 2023.

[4] A. Tuwalska, S. Grabska-Zielińska, and A. Sionkowska, "Chitosan/silk fibroin materials for biomedical applications—a review," Polymers (Basel)., vol. 14, no. 7, p. 1343, 2022.

[5] H. Liu et al., "A functional chitosan-based hydrogel as a wound dressing and drug delivery system in the treatment of wound healing," RSC Adv., vol. 8, no. 14, pp. 7533–7549, 2018.

[6] S. Narayana et al., "Potential benefits of using chitosan and silk fibroin topical hydrogel for managing wound healing and coagulation," Saudi Pharm. J., vol. 31, no. 3, pp. 462–471, 2023.

[7] P. Farshi et al., "Design, preparation, and characterization of silk fibroin/carboxymethyl cellulose wound dressing for skin tissue regeneration applications," Polym. Eng. Sci., vol. 62, no. 9, pp. 2741–2749, 2022.

[8] Z. Xu, T. Chen, K. Zhang, K. Meng, and H. Zhao, "Silk fibroin/chitosan hydrogel with antibacterial, hemostatic and sustained drug-release activities," Polym. Int., vol. 70, no. 12, pp. 1741–1751, 2021.

[9] M. Akrami-Hasan-Kohal, M. Eskandari, and A. Solouk, "Silk fibroin hydrogel/dexamethasone sodium phosphate loaded chitosan nanoparticles as a potential drug delivery system," Colloids Surfaces B Biointerfaces, vol. 205, p. 111892, 2021.

[10] L. Chan, Y. Lu, A. Taledaohan, Y. Wang, W. Wang, and Y. Wang, "A silk fibroin/chitosan hydrogel with ferulic acid derivatives: Promoting diabetic wound healing through immune modulation and angiogenesis," Int. J. Biol. Macromol., p. 146744, 2025.

[11] M. Dong et al., "Novel fabrication of antibiotic containing multifunctional silk fibroin injectable hydrogel dressing to enhance bactericidal action and wound healing efficiency on burn wound: in vitro and in vivo evaluations," Int. Wound J., vol. 19, no. 3, pp. 679–691, 2022.

[12] S. Khosravimelal, M. Chizari, B. Farhadihosseinabadi, M. Moosazadeh Moghaddam, and M. Gholipourmalekabadi, "Fabrication and characterization of an antibacterial chitosan/silk fibroin electrospun nanofiber loaded with a cationic peptide for wound-dressing application," J. Mater. Sci. Mater. Med., vol. 32, no. 9, p. 114, 2021.

[13] Z. Xu, E. Tang, and H. Zhao, "An environmentally sensitive silk fibroin/chitosan hydrogel and its drug release behaviors," Polymers (Basel)., vol. 11, no. 12, p. 1980, 2019.

[14] P. Heydari Foroushani et al., "Curcumin sustained release with a hybrid chitosan-silk fibroin nanofiber containing silver nanoparticles as a novel highly efficient antibacterial wound dressing," Nanomaterials, vol. 12, no. 19, p. 3426, 2022.

[15] Z. Suhail et al., "Controlled drug release and antibacterial properties of levofloxacin-loaded silk/chitosan green composite for wound dressing," Biomed. Mater. Devices, vol. 1, no. 2, pp. 796–804, 2023.

[16] Q. Min, D. Tian, Y. Zhang, C. Wang, Y. Wan, and J. Wu, "Strong and elastic chitosan/silk fibroin hydrogels incorporated with growth-factor-loaded microspheres for cartilage tissue engineering," Biomimetics, vol. 7, no. 2, p. 41, 2022.

[17] Y. Yu, X. Yu, D. Tian, A. Yu, and Y. Wan, "Thermo-responsive chitosan/silk fibroin/amino-functionalized mesoporous silica hydrogels with strong and elastic characteristics for bone tissue engineering," Int. J. Biol. Macromol., vol. 182, pp. 1746–1758, 2021.

[18] M. Haghighattalab, A. Kajbafzadeh, M. Baghani, Z. Gharehnazifam, B. M. Jobani, and M. Baniassadi, "Silk fibroin hydrogel reinforced with magnetic nanoparticles as an intelligent drug delivery system for sustained drug release," Front. Bioeng. Biotechnol., vol. 10, p. 891166, 2022.
[19] S. Deng et al., "Chitosan/silk fibroin nanofibers-based hierarchical sponges accelerate infected diabetic wound healing via a HClO self-producing cascade catalytic reaction," Carbohydr. Polym., vol. 321, p. 121340, 2023.
[20] Y. Kaptan, O. Karal-Yilmaz, B. Izbudak, B. Giray, B. Yilmaz, and A. Bal-Ozturk, "Preparation of tetracycline hydrochloride loaded chitosan/silk fibroin/ZnO antibacterial biocomposite hydrogel sponges for wound healing application," J. Polym. Res., vol. 30, no. 2, p. 49, 2023.
[21] V. Singh et al., "Silk fibroin hydrogel: A novel biopolymer for sustained release of vancomycin drug for diabetic wound healing," J. Mol. Struct., vol. 1286, p. 135548, 2023.
[22] M. Nazemoroaia, F. Bagheri, S. Z. Mirahmadi-Zare, F. Eslami-Kaliji, and A. Derakhshan, "Asymmetric natural wound dressing based on porous chitosan-alginate hydrogel/electrospun PCL-silk sericin loaded by 10-HDA for skin wound healing: In vitro and in vivo studies," Int. J. Pharm., vol. 668, p. 124976, 2025.
[23] S. He et al., "Heparinized silk fibroin hydrogels loading FGF1 promote the wound healing in rats with full-thickness skin excision," Biomed. Eng. Online, vol. 18, no. 1, p. 97, 2019.
[24] K. K. R. Ealla et al., "Doxycycline-integrated silk fibroin hydrogel: preparation, characterizations, and antimicrobial assessment for biomedical applications," BMC Oral Health, vol. 25, no. 1, p. 177, 2025.
[25] M. S. Pacheco, G. E. Kano, L. de Almeida Paulo, P. S. Lopes, and M. A. de Moraes, "Silk fibroin/chitosan/alginate multilayer membranes as a system for controlled drug release in wound healing," Int. J. Biol. Macromol., vol. 152, pp. 803–811, 2020.
[26] Q. Shi et al., "GMSC-derived exosomes combined with a chitosan/silk hydrogel sponge accelerates wound healing in a diabetic rat skin defect model," Front. Physiol., vol. 8, p. 904, 2017.
[27] M. H. Kazemi, S. Sajadimajd, and Z. G. Karaji, "In vitro investigation of wound healing performance of PVA/chitosan/silk electrospun mat loaded with deferoxamine and ciprofloxacin," Int. J. Biol. Macromol., vol. 253, p. 126602, 2023.